

# THE VALIDITY OF THE ADIABATIC CONTRACTION APPROXIMATION FOR DARK MATTER HALOS

ROLAND JESSEIT, THORSTEN NAAB, AND ANDREAS BURKERT  
 Max-Planck-Institut für Astronomie  
 Königstuhl 17, D-69117 Heidelberg, Germany  
 jesseit@mpia-hd.mpg.de, burkert@mpia-hd.mpg.de, naab@mpia-hd.mpg.de  
*Draft version October 23, 2018*

## ABSTRACT

We use high resolution numerical simulations to investigate the adiabatic contraction of dark matter halos with a Hernquist density profile. We test the response of the halos to the growth of additional axisymmetric disk potentials with various central concentrations and the spherically symmetric potential of a softened point mass. Adding the potentials on timescales that are long compared to the dynamical time scale of the halo, the contracted halos have density profiles that are in excellent agreement with analytical predictions based on the conservation of the adiabatic invariant  $M(r)r$ . This is surprising as this quantity is strictly conserved only for particles on circular orbits and in spherically symmetric potentials. If the same potentials are added on timescales that are short compared to the dynamical timescale, the result depends strongly on the adopted potential. The adiabatic approximation still works for disk potentials. It does, however, fail for the central potential.

*Subject headings:* dark matter — galaxies: formation — galaxies: halos

## 1. INTRODUCTION

The hierarchical clustering model is the paradigm for galaxy formation today. In this cosmological scenario, structure forms around peaks of primordial dark matter density fluctuations. The baryonic matter, which can dissipate energy through radiation, cools and falls into the center of its surrounding dark halo. The question of how a spherical mass distribution, e.g. a galactic bulge, will respond to the growth of mass in its center has been addressed by Barnes & White (1984), hereafter BW84. They devised a simple recipe for predicting the density profile of a contracted spherical density distribution. This recipe was used by Blumenthal et al. (1986) to examine contracted dark halos, assuming that the baryonic disk forms in the center so slowly that the time for the increase of mass inside an orbit of a dark particle is long compared to its orbital period. In a slowly varying potential the action integral  $j_i = \int p_i dq_i$  is a conserved property of the particle orbit, called an adiabatic invariant (Binney & Tremaine 1987). Here,  $j$  is the action,  $p$  and  $q$  are the phase space coordinates of the dark particle. As a first approximation, BW84 assumed a spherical density distribution with particles moving on circular orbits. In this case, the radial action integral simplifies to the conservation of angular momentum. With  $L = mvr$  and the circular velocity  $v^2(r) = GM(r)/r$  we get the adiabatic invariant  $M(r)r$ . Given that we know the final baryonic matter distribution, e.g. an exponential disk-like profile  $M_b(r)$  and the initial dark halo distribution  $M_i(r)$ , we can construct the final dark matter distribution  $M_f(r)$  according to

$$r_f[M_b(r_f) + M_f(r)] = rM_i(r), \quad (1)$$

where  $r_f$  is the final radius of a dark particle. This approximation is strictly valid only if the initial mass distribution is spherically symmetric. The mapping between initial and final radius is unique, because the dark particles are dissipationless and their circular orbits do not cross. The adiabatic compression has been used widely in estimating

rotation curves in semi-analytical galaxy models (Ryden & Gunn 1987; Ryden 1988, 1991; Flores et al. 1993; Mo, Mao, & White 1998), in investigating the origin of the Tully-Fisher relation (Courteau & Rix 1999), in analysing the core structure of dark matter halos (van den Bosch & Swaters 2001; Marchesini et al. 2002) and in the formation of gaseous disks in cosmological N-body halos (M. Steinmetz 2001, private communication). The adiabatic contraction assumption has been tested qualitatively in a low-resolution study by Blumenthal et al. (1986).

It is surprising that equation (1) should hold in realistic situations, where a non-spherical galactic disk is added to a halo of particles which move on eccentric or chaotic orbits (Valluri & Merritt 2000). In this paper we investigate the validity of equation (1), using high resolution numerical simulations. Adding a disk potential to an equilibrium N-body halo, we can study its reaction in the adiabatic limit, as well as for an abrupt change of the potential. In §2 we describe the model runs for different disk parameters and contraction times. In §3 we discuss the results and in §4 we draw our conclusions and present suggestions for future work.

## 2. THE SIMULATIONS

The N-body halo is set up according to the distribution function devised by Hernquist (1990, 1993). Its density distribution is  $\rho(r) = M_h r_h / [2\pi r(r + r_h)^3]$ , where  $M_h$  is the total mass and  $r_h$  is the scale length. The Hernquist halo has the same  $\rho \propto r^{-1}$  dependence in the center as the universal dark matter profile found by Navarro, Frenk, & White (1997), however with a finite total mass as the density in the outermost regions decreases as  $\rho \propto r^{-4}$ . The baryonic component is represented by analytic external potentials of a disk and a central point mass. We used the potential of an exponentially thin disk according to Dehnen & Binney (1998). Its strength depends on the ratio of the disk mass  $M_d$  to the disk scale length  $r_d$ . Fol-

lowing Navarro, Eke, & Frenk (1996), we started with a very large disk scale length and kept the disk mass constant throughout the simulation. The disk scale length is contracted linearly with time, where the contraction rate is a free parameter. Large contraction time scales compared to the dynamical time scales correspond to the adiabatic limit. In the limit of zero contraction time the halo will go through a phase of violent relaxation. The halo-disk system was allowed to relax after the contraction phase for several dynamical time scales. We applied a massive and a low-mass disk model with 20 % (MD) and 5 % (LD) of the total dark halo mass, and with a typical final scale length of  $0.14 r_h$ .

In order to test the dependence on the concentration of the potential we used a softened point mass potential following

$$\Phi_p(r) = \frac{GM_p \arctan(r/r_p)}{r_p}. \quad (2)$$

Similar to the disk case we kept its mass  $M_p$  constant and shrank the smoothing length to a final value of  $r_p = 0.03$  (test case PC). We also tested the case where  $r_p$  was kept constant and  $M_p$  was allowed to grow (PG). For all calculations we chose  $G = M_h = r_h = 1$ , where  $G$  is the gravitational constant. Simulations were performed with halos represented by  $N = 1 \times 10^4$ ,  $8 \times 10^4$ ,  $2 \times 10^5$  and  $1 \times 10^6$  particles in order to test the dependence of the results on the numerical resolution. All model parameters are listed in Table 1. The gravitational softening length  $\epsilon$  was chosen according to the criterium of Merritt (1996). We used a time step at least a hundred times smaller than the dynamical time scale we would expect at the half mass radius for each model. The timestep, adequate for the runs with the highest number of particles, was not enlarged for lower particle number runs. We used a newly developed tree code WINE (Wetzstein et al., in preparation) in combination with special purpose hardware GRAPE-5 (Kawai et al. 2000) at the MPA, Heidelberg. The refined force accuracy criterium of Salmon & Warren (1994) guarantees that the absolute force error stays below the precision of the GRAPE hardware.

### 3. RESULTS

The four top panels in Fig. 1 show the final density profiles of the contracted halos for two resolutions for the massive and the light disk, respectively (models LD1, LD2 and MD1, MD2). The error bars show the Poissonian error. The softening length is indicated with an arrow on each plot. In the innermost parts of the halo, i.e.  $r \leq 2\epsilon$ , the density is influenced by at least two effects: The softening length and fluctuations in the density due to small particle numbers. To show the effect of the fluctuations we plot the density profile of four consecutive dumps taken shortly after the contraction has been completed. This is important

as the fluctuations sometimes exceed the  $1 \sigma$  Poissonian error. At radii larger than two softening lengths the analytical approximation of BW84 gives a very good account of the matter distribution of the halo for every disk model. The two panels at the bottom of Fig. 1 show the point mass case which is also in very good agreement with the theoretical profile, independent of the way we grow the external potential. However, the density is somewhat lower than theoretically predicted inside the scale radius  $r_p$ .

Fig. 2 illustrates for the LD case that the agreement between numerical simulation and theoretical profile improves with increasing particle number, as we are able to probe deeper into the center of the dark matter halo.

In Fig. 3 we examine the response of the halo to an abrupt addition of the external potentials (models MDV, LDV and PV). The profile with the light disk (top left) still matches the theoretical curve. Even in the case of the massive disk (bottom left), the predicted density distribution agrees well with the numerical model although we find a somewhat lower density inside a radius of one disk scale length. Adding the point mass potential instantaneously (bottom right) leads to a density distribution that deviates strongly from the adiabatic prediction. The top right panel in Fig. 3 shows the time evolution of the 1% mass shell radius in each case. For the LD models the mass shells stabilize at more or less the same radius, though the detailed path of contraction is very different for LD2 and LDV. For the more centrally concentrated potential (PV) this is not the case. It stabilizes at radii further outside than in the adiabatic case. Consequently these density profiles are less concentrated in the center than in the adiabatic case.

### 4. CONCLUSIONS

We find that the adiabatic approximation is very robust in the parameter space that is occupied by normal spiral or dwarf galaxies. This remains valid even in cases where the contraction timescales are short compared with the dynamical time scales. Only for a point mass potential, a significant difference occurs. We conclude that the validity of the adiabatic approximation depends mainly on the concentration of the added potential. A better understanding of the underlying physics will require a detailed analysis of the orbital distribution of the particles prior and after the contraction phase. We will investigate this question in a subsequent paper.

A program to calculate disk potentials was kindly provided by Walter Dehnen. We want to thank Hans-Walter Rix, Matthias Steinmetz and Chris Gottbrath for helpful comments and discussions.

### REFERENCES

- Barnes, J. & White, S. D. M. 1984, MNRAS, 211, 753  
 Binney, J. & Tremaine, S. 1987, *Galaxy Dynamics*, (Princeton, NJ: Princeton University Press)  
 Blumenthal, G. R., Faber, S. M., Flores, R., & Primack, J. R. 1986, ApJ, 301, 27  
 Courteau, S. & Rix, H. 1999, ApJ, 513, 561  
 Dehnen, W. and Binney, J. 1998, MNRAS, 294, 429  
 Flores, R., Primack, J. R., Blumenthal, G. R., & Faber, S. M. 1993, ApJ, 412, 443  
 Hernquist, L. 1990, ApJ, 356, 359  
 Hernquist, L. 1993, ApJS, 86, 389  
 Kawai, A., Fukushima, T., Makino, J., & Taiji, M. 2000, PASJ, 52, 659  
 Marchesini, D., D’Onghia, E., Chincarini, G., Firmani, C., Conconi, P., Molinari, E., & Zaccari, A. 2002, ApJ, in press

- Merritt, D. 1996, *AJ*, 111, 2462
- Mo, H. J., Mao, S., & White, S. D. M. 1998, *MNRAS*, 295, 319
- Navarro, J. F., Eke, V. R., & Frenk, C. S. 1996, *MNRAS*, 283, L72
- Navarro, J. F., Frenk, C. S., & White, S. D. M. 1997, *ApJ*, 490, 493
- Ryden, B. S. 1988, *ApJ*, 329, 589
- Ryden, B. S. 1991, *ApJ*, 370, 15
- Ryden, B. S. & Gunn, J. E. 1987, *ApJ*, 318, 15
- Salmon, J. K. & Warren, M. S. 1994, *Journal of Computational Physics*, 111, 136
- Valluri, M. & Merritt, D. 2000, in *The Chaotic Universe, Proceedings of the Second ICRA Network Workshop*, Advanced Series in Astrophysics and Cosmology, vol.10, ed. V. G. Gurzadyan and R. Ruffini (World Scientific), 229
- van den Bosch, F. C. & Swaters, R. A. 2001, *MNRAS*, 325, 1017

TABLE 1  
MODEL RUNS

Model	Mass/scale length	N	$\epsilon$	dt [ $10^{-3}$ ]	type
LD1	0.05/0.14	$1 \times 10^4$	0.03	6.25	adiabatic
LD2	0.05/0.14	$2 \times 10^5$	0.007	6.25	adiabatic
LD3	0.05/0.14	$1 \times 10^6$	0.0035	6.25	adiabatic
LDV	0.05/0.14	$2 \times 10^5$	0.007	6.25	violent
MD1	0.2/0.14	$1 \times 10^4$	0.03	1.57	adiabatic
MD2	0.2/0.14	$2 \times 10^5$	0.007	1.57	adiabatic
MDV	0.2/0.14	$2 \times 10^5$	0.007	1.57	violent
PG	0.2/0.03	$8 \times 10^4$	0.01	0.78	point grow
PC	0.2/0.03	$8 \times 10^4$	0.01	0.78	point contract
PV	0.2/0.03	$8 \times 10^4$	0.01	0.78	point violent

Note. — Abbreviations for the model runs are LD = Light Disk, MD = Massive Disk, P = Point Mass, V = Violent, G = Mass Growth, C = Softening Length Contraction. Model parameters are N = number of particles and dt = integration time step. Second column shows mass to scale length ratios for point mass and disk models.

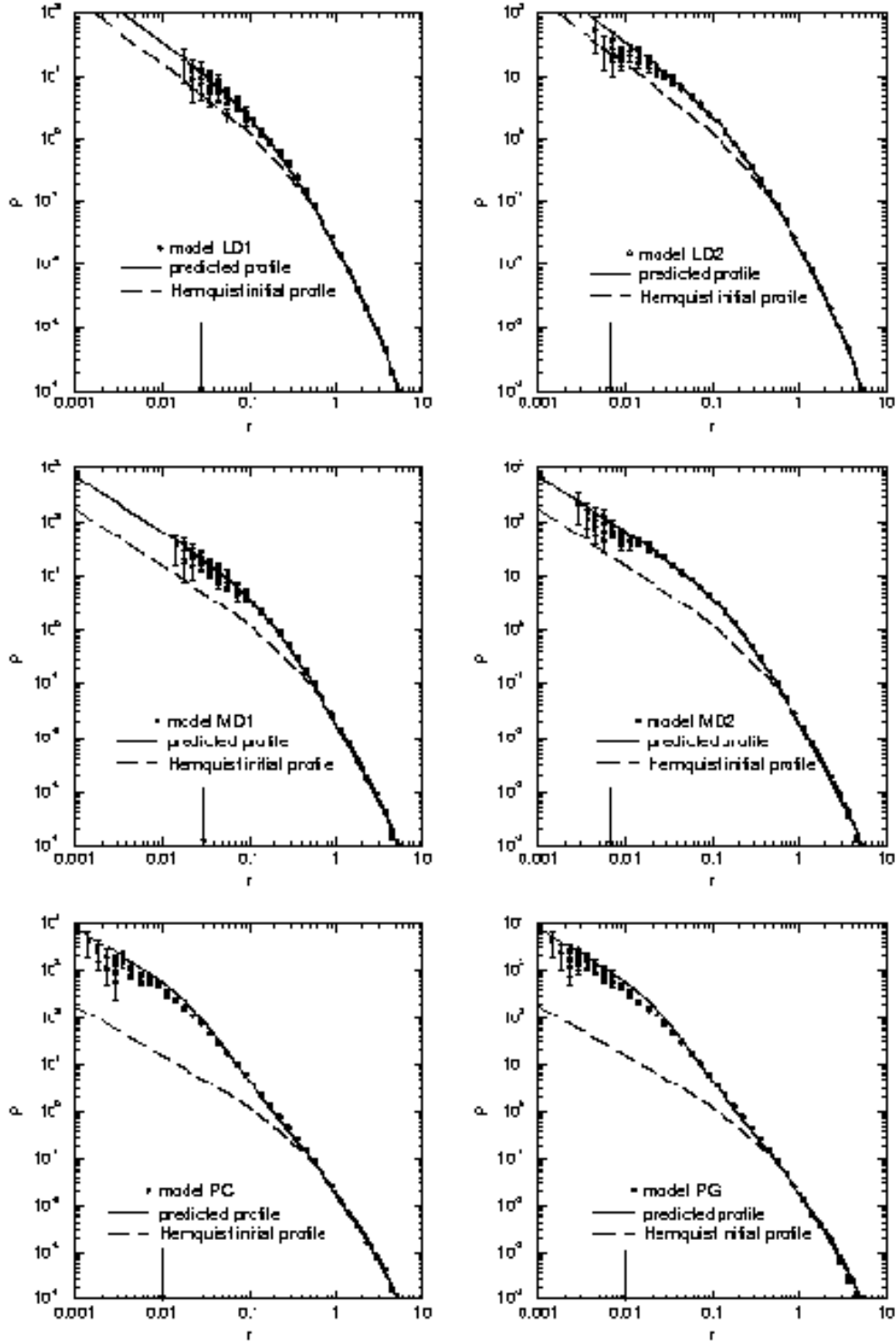


FIG. 1.— Final density profiles of contracted dark halos. The upper two panels show the results for the models LD1 and LD2, the following two for the models MD1 and MD2. The last two panels show the results for the point mass. In the left panel the contracting scale length case and in the right panel the growing mass case is shown. Arrows indicate the used softening length.

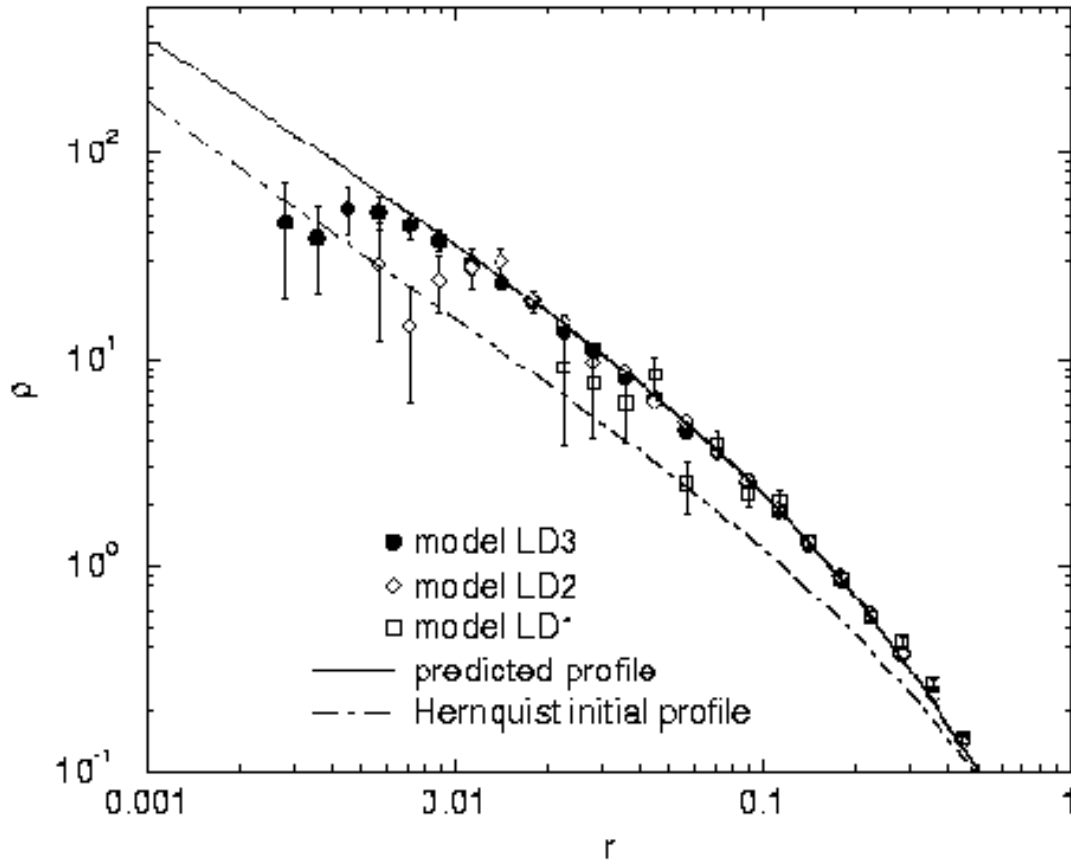


FIG. 2.— Final density profiles of LD1, LD2 and LD3 are shown to examine the effects of numerical resolution.

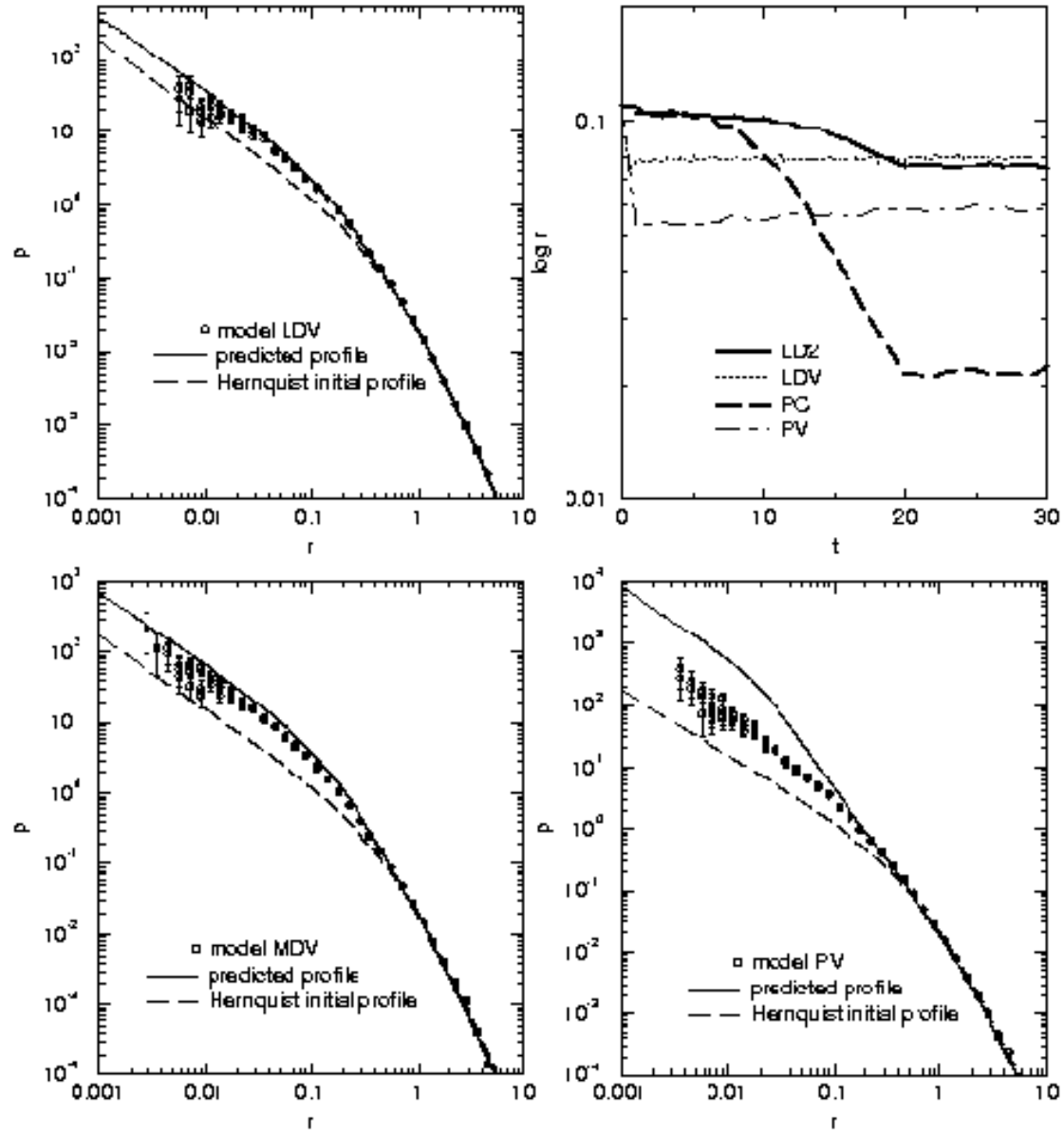


FIG. 3.— Final density profiles after abrupt addition of external potential. LDV top left, MDV bottom left and PV bottom right. In the top right panel a comparison of the evolution of the 1% mass shell radii between the adiabatic and the violent case of the models LD and P is shown.